JCTC Journal of Chemical Theory and Computation

Article

pubs.acs.org/JCTC

Improved Parameters for the Martini Coarse-Grained Protein Force Field

Djurre H. de Jong,[†] Gurpreet Singh,[‡] W. F. Drew Bennett,[‡] Clement Arnarez,[†] Tsjerk A. Wassenaar,[†] Lars V. Schäfer,[†] Xavier Periole,[†] D. Peter Tieleman,[‡] and Siewert J. Marrink*[,†]

[†]Groningen Biomolecular Sciences and Biotechnology Institute and Zernike Institute for Advanced Materials, University of Groningen, Nijenborgh 7, 9747 AG Groningen, The Netherlands

[‡]Department of Biological Sciences and Institute for Biocomplexity and Informatics, University of Calgary, 2500 University Dr. NW, Calgary, AB, Canada, T2N 1N4

Supporting Information

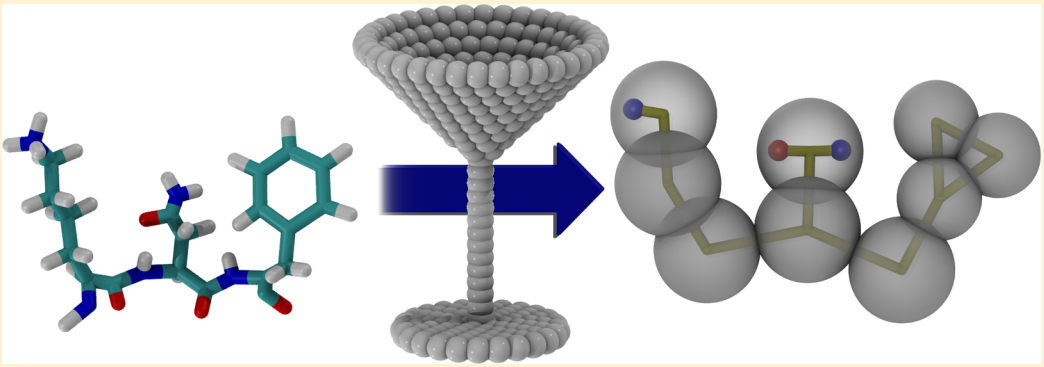

ABSTRACT: The Martini coarse-grained force field has been successfully used for simulating a wide range of (bio)molecular systems. Recent progress in our ability to test the model against fully atomistic force fields, however, has revealed some shortcomings. Most notable, phenylalanine and proline were too hydrophobic, and dimers formed by polar residues in apolar solvents did not bind strongly enough. Here, we reparametrize these residues either through reassignment of particle types or by introducing embedded charges. The new parameters are tested with respect to partitioning across a lipid bilayer, membrane binding of Wimley–White peptides, and dimerization free energy in solvents of different polarity. In addition, we improve some of the bonded terms in the Martini protein force field that lead to a more realistic length of α-helices and to improved numerical stability for polyalanine and glycine repeats. The new parameter set is denoted Martini version 2.2.

1. INTRODUCTION

The use of coarse-grained (CG) models in a variety of simulation techniques has proven to be a valuable tool used to probe the spatial and temporal evolution of systems on the mesoscale, beyond what is feasible with traditional all-atom (AA) models. A large diversity of coarse-graining approaches are available; they range from qualitative, often solvent-free models, via more realistic explicit solvation models, to models including chemical specificity (for recent overviews, see refs 1−5). Models within this latter category are typically parametrized based on comparison to atomistic simulations, using iterative Boltzmann,[6,7] force matching,[8,9] conditional reversible work,[10] or minimization of relative entropy[11] approaches. Our own model, coined the Martini force field,[12−14] has also been developed in close connection with atomistic models, especially considering the bonded interactions. However, the philosophy of our coarse-graining approach is different. Instead of focusing on an accurate reproduction of structural details at a particular state point for a specific system, we aim for a broader range of applications without the need to reparameterize the model each time. We do so by extensive calibration of the nonbonded interactions of the chemical building blocks against experimental data, in particular thermodynamic data such as oil/water partitioning coefficients, since processes such as lipid self-assembly, peptide-membrane binding, and protein−protein recognition depend critically on the degree to which the constituents partition between polar and nonpolar environments. The use of a consistent strategy for the development of compatible CG and atomic-level force fields is of additional importance for its intended use in multiscale applications.[15−19] The overall aim of our coarse-graining approach is to provide a simple model that is computationally fast and easy to use, yet flexible enough to be applicable to a wide range of (bio)molecular systems.

The name "Martini" for the force field was coined in 2007 with the release of version 2.0 for lipids.[13] The subsequent extension to peptides and proteins[14] was released as version

Received: July 25, 2012

   dx.doi.org/10.1021/ct300646g | J. Chem. Theory Comput. XXXX, XXX, XXX−XXX

2.1. The Martini model is based on an approximate four-to-one mapping; i.e., on average, four heavy atoms plus associated hydrogens are represented by a single interaction center, with an exception for ring-like molecules. The mapping of ring-like fragments or small molecules (e.g., benzene, cholesterol, and several of the amino acid side chains) is not possible with the general four-to-one mapping approach. Such molecules are therefore mapped with a higher resolution of up to two-to-one. The Martini model considers four main types of interaction sites: polar (P), nonpolar (N), apolar (C), and charged (Q). Within a main type, subtypes are distinguished either by a letter denoting the hydrogen-bonding capabilities (d = donor, a = acceptor, da = both, 0 = none) or by a number indicating the degree of polarity (from 1 = low polarity to 5 = high polarity). Small (ring-type) particles are denoted with a prefix "S". To improve the treatment of electrostatic interactions, polarizable water models were also recently introduced for use with Martini.[20,21]

Currently, the Martini force field provides parameters for a variety of (bio)molecules, including many different lipids,[12,22] sterols,[13,23] peptides and proteins,[14] sugars,[24,25] polymers,[26−29] DNA,[30] nanoparticles,[31−33] dendrimers,[34,35] and more. The list of applications of the Martini model to date is broad, reflecting the flexibility and transferability underlying our coarse-graining protocol. Some recent applications include protein mediated vesicle fusion;[36−38] membrane domain formation;[39−46] lipid flip-flopping;[47,48] lipid and surfactant phase behavior;[49−54] the collapse of lipid monolayers;[55−57] membrane tether formation;[58] peptide- and protein-induced membrane remodeling;[59−71] the self-assembly and lipid sorting of membrane proteins;[72−89] gating and conformational changes of membrane proteins;[90−96] protein adsorption on solid supports;[97,98] mechanical properties of protein filaments;[99,100] aggregation of peptides,[101−103] peptide amphiphiles,[104] and amyloid fibrils;[105,106] nanopore imbibition and surface wetting;[107,108] membrane translocation and lipid adhesion of nanoparticles;[31,34,109−115] membrane engineering;[116] polymer induced membrane adhesion and tethering;[117−119] nanocoating of a polymer matrix;[120] protein−ligand binding;[121] structure and dynamics of lipoprotein particles and nanodiscs;[122−127] lipoplexes;[128] and drug-delivery systems.[129−134] Note, variations of the Martini protein force field have been developed independently by the groups of Sansom[135] and Schulten.[136]

Recently, progress in computational power has allowed for more extensive testing of the Martini force field with respect to all-atom models. Singh and Tieleman[137] compared relative binding free energies of the Wimley−White (WW) pentapeptides to an experimentally derived free energy scale. Overall, the Martini model predicts the relative binding of these peptides to a lipid membrane in close agreement with the experimental data,[138] with notable exceptions for the charged residues, as well as phenylalanine and proline. The first category can be improved by resorting to the polarizable water model, but both phenylalanine and proline are apparently too hydrophobic. de Jong et al.[139] studied the dimerization free energy of amino acid side chains in solvents of different polarity. Here, also the overall performance of Martini is quite good in comparison to all-atom force fields such as Gromos and OPLS. Again, exceptions are the aromatic side chains, which are too hydrophobic. In addition, charged and polar interactions in a low dielectric medium are too weak compared to the atomistic models. Furthermore, ongoing refinement of partitioning free energy profiles across a water/bilayer interface by MacCallum et al.[140] reveals a significantly underestimated interfacial binding of the polar side chains asparagine and glutamine in Martini.

In the current work, we aim to fix some of these shortcomings, largely pertaining to the protein force field. These include (*i*) new topologies for proline, phenylalanine, and tryptophan side chains to improve partitioning free energies; (*ii*) introduction of an off-center charge model for a more realistic description of contact pairs of oppositely charged residues; (*iii*) parametrization of polarized beads for polar side chains to improve dimerization in apolar environments and interfacial binding; and (*iv*) some adjustment of bonded terms to improve the length of standard α-helices and increase numerical stability for polyalanine and glycine repeats. The new version of the force field will be denoted Martini 2.2 (or 2.2P in combination with the polarizable water model).

The rest of this paper is organized as follows. In section 2, the methods are outlined, providing details about the simulation setups used for refining the parameters. In section 3, the results are presented, subdivided into sections dealing with apolar residues (Phe, Trp, Pro), then charged (Glu, Asp, Arg, Lys, His) and polar ones (Thr, Ser, Asn, Gln, His), followed by a section on the bonded terms and a section on the new script used for implementation. A short conclusive paragraph ends this paper.

2. METHODS

2.1. General. The molecular dynamics (MD) simulations described in this work were performed using the GROMACS software package,[141] version 4.x. The scheme developed for the Martini model[12−14] was used: nonbonded interactions are cut off at a distance of 1.2 nm with smooth switching of the interactions and forces from 0.0 to 1.2 nm for the Coulomb potential and 0.9 to 1.2 nm for the Lennard-Jones (LJ) potential. The pair-list update frequency was set to once per 10 steps. A time step of 20−30 fs was used in most cases, which is adequate for preserving energy and temperature in Martini simulations.[142] Note, the simulation times reported in the manuscript are plain simulation times. Constant temperature and pressure was maintained using weak coupling to a bath.[143] Standard input files as well as the newly developed parameters can be downloaded from http://cgmartini.nl.

2.2. Partitioning Free Energy. Potentials of mean force (PMFs) for amino acid side chain analogues (SCAs) across a DOPC (dioleoyl-phosphatidylcholine) bilayer were calculated using umbrella sampling as described in MacCallum et al.[140] Small bilayer patches were simulated with 72 DOPCs, 1200 water beads, and one side chain. Polarizable water was used in cases of polar/charged side chains. For each PMF, we ran 81 independent simulations with a harmonic restraint on the distance between the side chain and the center of the DOPC bilayer in the z dimension. The distance was varied from −4 to +4 nm with an 0.1 nm spacing and a 1000 kJ mol^{-1} nm^{-2} force constant. Each simulation was run for 100 ns. The weighted histogram analysis method (WHAM)[144] was used to calculate the free energy profiles.

Partitioning free energies of SCAs between water and oil (decane) were calculated using thermodynamic integration. Separate boxes with a single SCA solvated by 334 CG water beads or 122 decane molecules were set up. In both solvents, 2 ns simulations were run at each lambda point, using 11 equally spaced points. The electrostatic and van der Waals interactions were switched off separately when charged molecules were present in the system. The free energies and the corresponding

errors were calculated using the Bennett Acceptance Ratio as implemented in the g_bar analysis tool of GROMACS. The partitioning free energy, ΔG^{part}, was obtained by subtracting the free energy in oil from the free energy in water.

2.3. Dimerization Free Energy. The dimerization free energy, ΔG^{dim}, of pairs of amino acid SCAs was computed as described by de Jong et al.[139] We prepared systems consisting of two amino acid SCAs solvated in a cubic unit cell with an edge length ~3.0 nm, filled with either water or decane. For each pair considered, we determined the PMF as a function of the side chains' center of mass (COM) distance. Simulations were run with the COM distances between SCAs constrained in the range 0.3−1.5 nm with a 0.025 nm interval. At each distance the system was simulated for 2 ns from which the first 50 ps were discarded as an equilibration period. Over the remaining simulation time, the mean constraining force was calculated using the constraint pulling code implemented in GROMACS and integrated as described by Hess.[145] From these PMFs, the dimerization free energy, ΔG^{dim}, was obtained using[146]

$$\Delta G^{\mathrm{dim}} = -k_{\mathrm{B}}T \ln\left(\frac{4\pi R_{\mathrm{max}}^3 \int_0^{r_c} r^2 g(r)\,\mathrm{d}r}{3v^{\circ}\int_{r_c}^{R_{\mathrm{max}}} r^2 g(r)\,\mathrm{d}r}\right) \quad (1)$$

where k_{B} is the Boltzmann constant, T is the simulation temperature, r is SCAs' COM distance, r_c is the dimer−monomer cutoff (defined by the distance at which the PMF reaches its first maximum), R_{max} is the maximum distance considered, v° is the standard volume (1.66 nm^3, equivalent to 1 mol L^{-1}), and $g(r)$ is the radial distribution function which is calculated from the PMF using

$$g(r) = \mathrm{e}^{-\mathrm{PMF}(r)/k_{\mathrm{B}}T} \quad (2)$$

Statistical errors were calculated using a Monte Carlo procedure: 10 000 PMF profiles were generated using mean and standard deviation of the constraining force for every distance, r. For all profiles, ΔG^{dim} is subsequently calculated using eq 1, and the mean and standard error are obtained.

2.4. Binding of WW Peptides. Wimley−White (WW) peptides are pentapeptides of fixed sequence Ac-WLXLL, where X denotes a variable residue. The binding of these peptides to a POPC (palmitoyl-oleoyl-PC)/water interface was studied experimentally.[138] The relative binding free energies $\Delta\Delta G^{\mathrm{WW}}$ of these peptides with respect to X = Ala provides an energy scale that is useful as a yardstick to gauge the relative surface affinity of different residues. Here, we calculated $\Delta\Delta G^{\mathrm{WW}}$ to test our new parameters using a protocol recently established by Singh and Tieleman.[137] In short, for amino acids Phe, Trp, and Pro, the $\Delta\Delta G^{\mathrm{WW}}$ is obtained using a combination of free energy perturbation (FEP) and multiple Bennett acceptance ratio (MBAR) methods, following the thermodynamic cycle as described in detail elsewhere.[137] For polar residues, the PMF profiles for translocating the entire peptide from the interface to the bulk water were computed using the distance between the COM of the POPC bilayer and the COM of the peptide as the reaction coordinate. The COM of the peptide was held at its relative position by applying a harmonic potential with a force constant of 1000 kJ mol^{-1} nm^{-2}. After an initial equilibration, data were collected over 600−1200 ns time periods depending on the convergence of the PMFs. In some cases, multiple simulations were performed to collect better statistics. The data were divided into windows of 100 ns to compute the free energies and standard errors, using the weighted histogram analysis method (WHAM) as implemented[147] in GROMACS. The free energy of adsorption of residue X at the interface from the bulk was calculated as

$$\Delta G^{\mathrm{WW}}(\mathrm{X}) = -k_{\mathrm{B}}T \ln\left[\int_{Z_f}^{Z_s} \mathrm{e}^{-\Delta G(z)/k_{\mathrm{B}}T}\,\mathrm{d}z\right] \quad (3)$$

where z_s = 1.0 nm and z_f = 4.0 nm define the limit of the POPC/water interface and bulk water, respectively. The integrations were carried out numerically using Simpson's rule. The relative binding free energy of residue X, $\Delta\Delta G^{\mathrm{WW}}(\mathrm{X})$, is obtained by subtracting $\Delta G^{\mathrm{WW}}(\mathrm{Ala})$ from $\Delta G^{\mathrm{WW}}(\mathrm{X})$.

3. RESULTS

3.1. Change of Amino Acid Particle Type for Phe, Trp, and Pro. On the basis of dimerization data of amino acid side chain analogues[139] and interfacial binding of Wimley−White (WW) peptides,[137] it has become clear that especially Phe and Pro, and to a lesser extent Trp, are too hydrophobic in the Martini 2.1 force field.

For Phe, the behavior can be greatly improved by changing the particle type from SC4 to the slightly more polar SC5. As shown in Table 1, the dimerization free energy in aqueous solution (ΔG^{dim}, water) increases from −4.5 kJ mol^{-1} to −3.0 kJ mol^{-1}, which is in better agreement with the value of −1.6 kJ mol^{-1} predicted using atomistic models.[139] The dimerization free energy in less polar solvents (ΔG^{dim}, oil) is hardly affected. The relative binding free energy of the WW peptide ($\Delta\Delta G^{\mathrm{WW}}$) also improves and gets within $k_{\mathrm{B}}T$ of the experimental value, see Table 1. The partitioning of the Phe side chain analogue across the water/bilayer interface was also computed. In Figure 1, the results for the original SC4 particle type and the new SC5 particle type are compared. The latter shows an improved overall binding profile. For consistency, we also investigated the use of the SC5 particle type to model benzene (note, in Martini benzene and Phe SCA are represented the same way). The original model[13] underestimates the partitioning of benzene in water; the partition free energy of benzene between butane and water is 22 kJ mol^{-1} compared to the experimental value[148] of 12.4 kJ mol^{-1} (using cyclohexane). With the new model, the value drops to 10 kJ mol^{-1}, slightly too hydrophilic. Note that the properties of pure benzene solvent are not affected by the change of particle type. The SC5 self-interaction is identical to the SC4 self-interaction (see the full interaction matrix[13]).

Although Trp performs quite well in the Martini 2.1 parametrization, the properties can actually be somewhat improved using a similar particle reassignment as for Phe. In changing the original SC4-SC4-SC4-SP1 to SC5-SC5-SC4-SNd, ΔG^{dim} (water) changes from −4.7 kJ mol^{-1} to −4.0 kJ mol^{-1}, compared to the atomistic value[139] of −3.3 kJ mol^{-1}. The added benefit of the new particle assignment is the presence of an explicit hydrogen bond donor group (SNd), which better reflects the underlying chemical nature of the Trp side chain. Considering the WW peptides, the new particle assignment for Trp does not change the already good agreement with the experimental binding free energy (see Table 1). The partitioning profile along the bilayer normal shows significant improvement, in line with the results obtained for Phe (Figure 1). For the other aromatic residues, His and Tyr, the agreement between atomistic data and the Martini

dx.doi.org/10.1021/ct300646g | J. Chem. Theory Comput. XXXX, XXX, XXX−XXX

Table 1. Overview of Parameters and Thermodynamic Properties of Amino Acid Side Chain Analogues[a]

SC		type (charge)[b]	$\Delta\Delta G^{WW}$ [c]	ΔG^{part} [d]	ΔG^{dim} water[e]	ΔG^{dim} oil[e]
Phe	ref.		5.4 ± 0.3	12	−1.6	−2.9
	CG	*SC4-SC4-SC4*	12.2 ± 0.1	21	−4.5	−1.3
		SC5-SC5-SC5	7.7 ± 0.1	10	−3.0	−1.7
Trp	ref.		8.5 ± 0.4	9	−3.3	−3.3
	CG	*SC4-SP1-SC4-SC4*	9.2 ± 0.1	10	−4.7	−3.0
		SC4-SNd-SC5-SC5	9.4 ± 0.1	8	−4.0	−2.7
Pro[f]	ref.		−1.2 ± 0.6			
	CG	*Na-AC2*	7.6 ± 0.1	20		
		P4-AC2	4.1 ± 0.1	20		
		P4−C3	1.9 ± 0.1	12		
		P4−C5	0.7 ± 0.1	9		
Thr	ref.		0.1 ± 0.4	−11	0.2	−5.8
	CG	*P1*	−1.9 ± 0.1	−12	0.0	−2.3
		N0 (0.36)	−0.3 ± 0.3	−12	−0.5	−4.0
		Nda (0.31)	2.3 ± 0.3	−13	−0.5	−4.2
Ser	ref.		0.2 ± 0.4	−14	1.6	−5.9
	CG	*P1*	−1.9 ± 0.1	−12	0.0	−2.3
		N0 (0.40)	−0.5 ± 0.3	−14	−0.2	−5.2
Asn	ref.		−1.0 ± 0.4	−28	−0.1	−17.3
	CG	*P5*	−2.7 ± 0.1	−31	0.3	−4.2
		Nda (0.51)	1.9 ± 0.7	−28	−0.2	−20.6
		Nda (0.46)	2.0 ± 0.4	−23	−0.4	−13.9
		N0 (0.54)	−1.3 ± 0.3	−27	−0.2	−18.1
Gln	ref.		−1.7 ± 0.4	−25	−1.2	−17.2
	CG	*P4*	−2.0 ± 0.1	−23	−0.1	−3.4
		Nda (0.42)	2.4 ± 0.2	−20	−0.2	−7.2
		N0 (0.51)	−1.1 ± 0.5	−24	−0.6	−14.6
His+	ref.				1.0	
	CG	SC4-SP1-SQd		−66	0.4	
		SC4-SP1-SQd (off-center)		−90	0.5	
Lys	ref.		−4.2 ± 0.7		1.0	
	CG	*C3-Qd*	−3.6 ± 0.1	−55	0.7	
		C3-Qd (off-center)	−3.0 ± 0.3	−73	0.2	
Glu	ref.		−7.7 ± 0.5		1.7	
	CG	*Qa*	−5.2 ± 0.1	−71	4.7	
		Qa (off-center)	−7.2 ± 0.3	−88	4.0	
Arg	ref.		−3.4 ± 0.7		1.5	
	CG	*N0-Qd*	−3.0 ± 0.1	−70	−0.2	
		N0-Qd (off-center)	−2.5 ± 0.3	−89	0.2	
Asp	ref.		−4.4 ± 0.4		3.9	
	CG	*Qa*	−5.3 ± 0.1	−71	4.7	
		Qa (off-center)	−6.4 ± 0.4	−88	4.0	

[a]Binding free energy difference $\Delta\Delta G^{WW}$ of Wimley−White peptides to a POPC/water interface, partitioning free energy ΔG^{part} between water and oil, and dimerization free energy ΔG^{dim} in either water or oil. All values in kJ mol^{-1}. Standard errors for $\Delta\Delta G^{WW}$ are indicated; standard errors are about 1 kJ mol^{-1} for ΔG^{part} and about 0.1 kJ mol^{-1} for ΔG^{dim}. [b]Italic font denotes results for Martini 2.1; bold font is used for the final set of parameters of Martini 2.2. In cases of polar and charged residues, data are obtained using the polarizable water model and Martini 2.2P. Reference (ref.) data from the sources in footnotes *c*−*e*. [c]Experimental values[138] with partitioning free energy of Ala set to zero. [d]Experimental data.[149,150] [e]Atomistic MD data.[139] [f]In case of Pro, the first CG particle type is for the backbone.

force field is already quite good, and no further improvement was attempted.

In the case of Pro, a number of different particle assignments were tried, also involving the backbone bead. We focused on improving the WW peptide binding free energy. Results are shown in Table 1 for a number of particle combinations. It is clear that the original assignment Na-AC2 is too hydrophobic, and much better results are obtained, increasing the polarity of the backbone and/or the polarity of the side chain. On the basis of the arguments that (*i*) the backbone polarity should be less than that of a regular amino acid due to the reduced H-bonding propensity and (*ii*) the side chain analogue is actually propane that should be kept rather apolar, we settled on the P4−C3 combination. Note that the P4 particle type for the Pro backbone only applies to the case where the residue is part of an unstructured chain. As part of α-helix or β-strand, less polar particle types are used (see ref 14) which remain valid in Martini 2.2.

In summary, we reparameterized the residues Phe, Trp, and Pro, improving their self-association behavior, binding of the respective pentapeptides, and partitioning across the membrane. The new particle types are highlighted in bold in Table 1. Future tests should reveal whether or not these parameters lead to a generic improvement.

3.2. Improving Charged Residues by Putting the Charge Off-Center. The absence of partial charges in the standard Martini water model warrants the use of a global screening constant of ε_r = 15. Together with the smooth shifting of the electrostatic interaction toward the cutoff (1.2 nm), this treatment results in a distance dependent dielectric screening. However, charged particles feel the same screening independent of their environment. Consequently, charge−charge interactions in an apolar medium are severely underestimated. This effect becomes evident from Figure 2, which shows the PMFs for the association of the Lys−Lys and Lys−Glu pairs in an apolar solvent, both for Martini and two atomistic models. In Martini 2.1, a relatively shallow contact pair is observed for oppositely charged residues, whereas the atomistic force fields show very strong binding. In contrast, Martini 2.1 predicts a stable contact pair for like charged residues, at odds with the global repulsion seen with the more detailed models.

Improvement of this unphysical situation is obtained using the polarizable Martini water model (compare PMFs with Martini 2.1 to 2.1P in Figure 2). The Lys−Lys contact pair disappears, and the Lys−Glu binding strength increases. However, Coulombic interactions fall off as $1/r$, and thus the bigger size of the CG beads (defined by their van der Waals radius, ∼0.26 nm) limits the approach of the charged beads to ∼0.5 nm, whereas in atomistic models the charges can come much closer. Therefore, the interaction strength between the charged atomistic side chains is still much stronger.

To remedy this issue, we designed an alternative model for charged side chains in which the electrostatic and van der Waals interactions are carried by two different particles. The two particles are connected by a constrained bond of length 0.11 nm, as illustrated in Figure 3, and have a mass of 36 amu. Using this off-center setup, the charges may come closer, and the interaction increases by approximately a factor of 3 in the case of the Lys−Glu pair (compare Martini 2.1P to 2.2P in Figure 2). The Lys−Lys pair, for which close contact of charges is not favorable, is not further improved.

dx.doi.org/10.1021/ct300646g | J. Chem. Theory Comput. XXXX, XXX, XXX−XXX

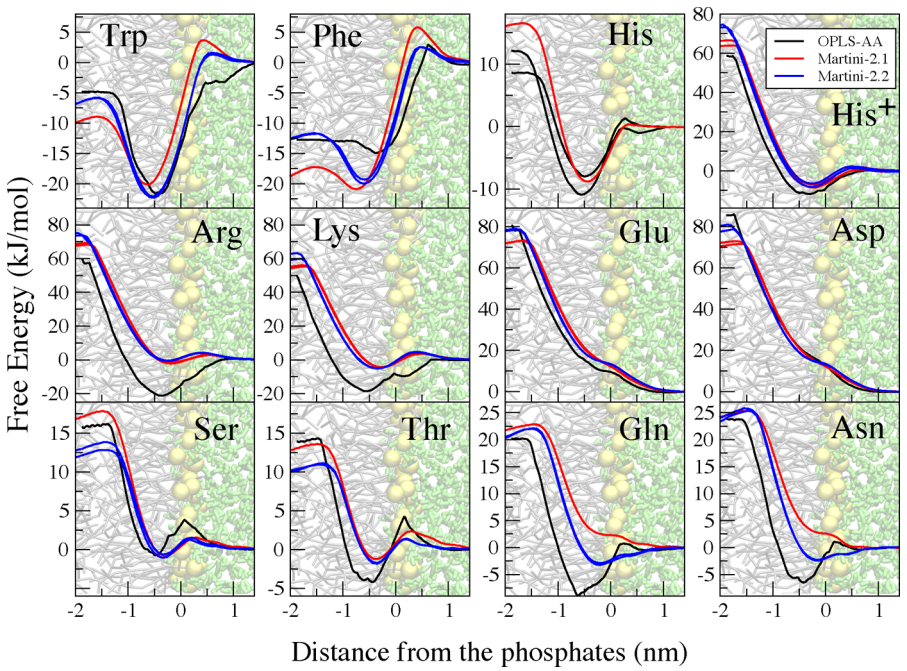

Figure 1. Potentials of mean force (PMF) for side chain analogues across a DOPC bilayer interface. Each PMF was set to 0 kJ mol^{-1} in bulk water and to 0 nm at the peak in the phosphate density for each bilayer. In the background, one leaflet of the DOPC bilayer is shown, with the lipids depicted as gray lines, water as green lines, and the phosphate beads shown by yellow spheres. Black lines denote results obtained with the OPLS all-atom force field and red/blue lines with Martini 2.1/2.2. In the case of polar and charged side chains, Martini 2.1P/2.2P is used. PMFs obtained with the Martini 2.2 models were obtained for both leaflets and are shown as independent profiles to give an estimate of the accuracy. PMFs for neutral His modeled with the OPLS force field are obtained for both the δ and ε protonated form (δ protonated has the lowest energy at the bilayer midplane).

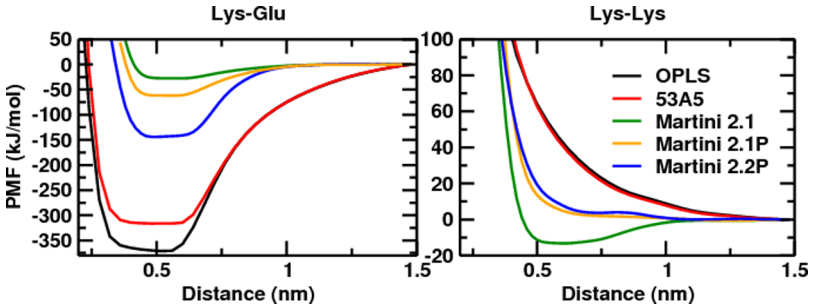

Figure 2. Potential of mean force (PMF) for Lys−Glu (left) and Lys−Lys (right) in decane. PMFs are plotted against the center of mass distance between the side chain analogue pairs. Black/red lines are obtained with the atomistic force fields OPLS/GROMOS, green/orange/blue lines with Martini 2.1/2.1P/2.2P. Errors do not exceed the thickness of the lines.

The new parameters do not change the already good behavior observed with Martini 2.1P in regard to the partitioning of the charged particles along the bilayer interface (Figure 1). The same is true for the binding of the WW peptides, for which the relative binding free energy is reproduced to within 1 k_BT from the experimental values for the charged residues in both Martini 2.1P and 2.2P (Table 1). Dimerization free energies of charged residues in water remain also largely unaffected and in overall good agreement with the atomistic data (Table 1).

For histidine, the charged form had not been parametrized for Martini 2.1.[14] Following the general pattern used for the other charged amino acids in Martini 2.1 and using the topology of neutral His, we defined a side chain topology for His+ consisting of a three bead ring: SC4-SP1-SQd. The bonded interactions are unchanged compared to the neutral form, the SC4 bead is bound to the protein backbone, and the SQd bead carries a +1 e charge. In addition to this topology in line with the Martini 2.1 force field, we also defined a topology for His+ where the charge was placed off-center. Both His+ topologies have a strongly negative oil/water partitioning free energy (−66 and −90 kJ mol^{-1}, respectively) and show very similar membrane partitioning behavior (Figure 1) and dimerization free energies in water and decane consistent with the atomistic data (cf. Table 1).

We conclude that the charge off-center setup describes the behavior of charged residues at the distance of contact more realistically. In particular, there is a drastic improvement of the SCA dimerization free energy in solvents of low polarity. The off-center model will be set as the default in Martini 2.2P (Table 1). Whether or not this approach could also improve the description of other charged beads in Martini (e.g., lipid head groups) remains to be tested.

dx.doi.org/10.1021/ct300646g | J. Chem. Theory Comput. XXXX, XXX, XXX−XXX

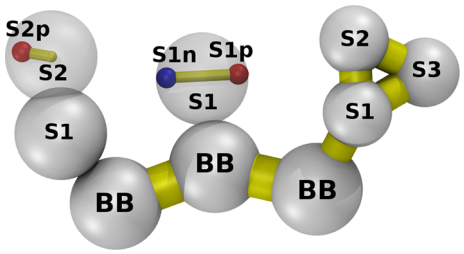

Figure 3. Schematic drawing of a Lys−Asn−Phe peptide demonstrating the new topologies for charged and polar amino acids in Martini 2.2P. As an example of charged residues, the Lys side chain consists of two beads, S1 and S2, carrying the van der Waals interaction. An additional bead is introduced, S2p, which carries the full positive charge of Lys but has no van der Waals interaction. It is bound to S2 using a 0.11 nm constraint. For polar residues like Asn, the side chain consists of one main particle S1 carrying the van der Waals interaction. It is a virtual site positioned in the middle of two additional sites S1n and S1p that carry a negative and a positive partial charge and no van der Waals interaction. Their mutual distance is constrained at 0.28 nm. The topology of aromatic residues like Phe consists of three beads S1, S2, and S3 and remains identical to the topology in Martini 2.1. For each side chain, the S1 particle is bonded to the peptide backbone bead (BB).

3.3. Improving Polar Residues Using Polarized Particles. Just like interactions between charged beads, interactions between polar particles (P type) in an oil-like medium are grossly underestimated in the Martini force field. This is evident from the dimerization free energies of the side chain analogues in decane (cf. Table 1). In contrast to charged particles, the absence of any charge in polar particles leaves them blind to changes in electrostatic screening, and thus the use of a polarizable water model has no effect. Alternatively, we introduce embedded dipoles to polar residues, in line with the polarizable Martini water model. Figure 3 shows the typical setup of a "polarized" residue. It consists of one virtual site and two real sites. The virtual site is the center of the LJ interactions and is defined as the geometrical center of the two real sites. The real sites carry equal partial charges of opposite sign and interact via a Coulomb potential, except between each other. They do not have LJ interactions. Both have a mass of 36 amu and are bound to each other by a 0.28 nm constraint. This bond defines a fixed dipole moment that can thus only contribute to orientational polarization, in contrast with the case of polarizable Martini water where the charges can move independently. The magnitude of the embedded charges is used as a fitting parameter, together with the particle type of the virtual site which determines the strength of the LJ interactions. The resulting dipole moment therefore has no direct physical meaning. Due to the addition of electrostatic interactions, the contribution from the LJ interactions is reduced compared to the standard Martini model.

We fitted the parameters in the first instance by reproducing the experimental oil/water partitioning free energies. The results for a number of combinations of charges and bead types are given in Table 1. The partitioning free energies are very sensitive to the magnitude of the charges. For Thr and Ser, charges in the range 0.3−0.4 e match the experimental data. For Asn and Gln, slightly bigger charges of 0.4−0.55 e are required, reflecting the higher polarity of these side chains.

We computed the dimerization free energy of polar SCA pairs using the polarized particle type. Results are also shown in Table 1 and compared to values obtained with atomistic force fields. It is evident that the self-association of each of the polar residues in an apolar solvent (ΔG^{dim}, oil) is improved. In particular, Asn switches from a weak (around 4 kJ mol^{-1}) to a strong (14−20 kJ mol^{-1}) type of association, which is consistent with the atomistic data. The dimerization of Thr and Ser also improves by about 2−3 kJ mol^{-1}. Self-association in an aqueous environment (ΔG^{dim}, water) is largely unaffected and remains in good agreement with the atomistic data for all polar side chains. Similar ΔG^{dim} can be obtained with Nda and N0 particle types by increasing the dipole charges in N0 compared to Nda.

We further tested the polarized side chains by considering their partitioning behavior across a lipid membrane. The PMFs of the respective SCAs are shown in Figure 1 and are compared to previous results obtained using an atomistic model and Martini 2.1. The profiles for Thr and Ser match the atomistic data very well, as does the nonpolarized version of Martini. In fact, Martini 2.1 is slightly better in that respect. For Asn and Gln, however, the profiles significantly improve. Notably the free energy minimum at the water/lipid interface is now reproduced, although it is still too shallow. Asn and Gln require the use of an Nda particle type to observe this minimum. In the case of Ser/Thr, the N0 particle type is appropriate.

Finally, the binding free energy of the WW peptides, $\Delta\Delta G^{\mathrm{WW}}$, was calculated using the polarized side chains. The results are given in Table 1. Overall, Martini 2.1 predicts too weak binding of these pentapeptides as compared to the experimental data, although the differences are less than $k_{\mathrm{B}}T$. Perfect agreement can be obtained in the case of Ser and Thr using a polarized particle of N0 type. For Asn and Gln, the N0 particle also gives the best results. As discussed above, the Nda particle that is needed to reproduce the interfacial minimum of the PMFs across the membrane actually results in too strong binding of the respective pentapeptides by about 1.5 $k_{\mathrm{B}}T$.

The art of coarse-graining is in the compromise: one cannot always get everything right at the same time. Here, in the case of Asn and Gln side chains, we decide to give priority to the partitioning profiles along the membrane normal, which show that Gln and Asn bind strongly at the lipid/water interface. This feature is only reproduced using an Nda particle type. One may argue that the relative weak binding of the Gln and Asn pentapeptides, suggested by the experimental data from Wimley and White, is caused by the restricted orientational freedom of the central residues. Whereas a free Asn or Gln SCA can align its hydrophobic moment along the membrane normal, as part of a pentapeptide this is not possible, providing a possible explanation for the reduced binding strength.

We also tested the use of polarized particles for the neutral form of histidine. However this change did not improve the partitioning behavior over the membrane (data not shown), while the oil/water partitioning free energy deviated significantly more from the experimental value as compared to Martini 2.1. For the topology with the best cross bilayer profile (SC4-SP1-SNda with ±0.20 e partial charges), the partitioning free energy was −15 kJ mol^{-1} versus the −20 kJ mol^{-1} experimentally obtained. The neutral form of His was not tested with respect to WW peptides and dimerization free energies. For these reasons, we decided to leave the neutral His topology unchanged with respect to Martini 2.1.

In summary, in this section, we introduced the concept of polarized particles to remedy some of the shortcomings of polar residues in Martini. The final set of parameters is highlighted in bold in Table 1. Due to the addition of charged interaction

sites, the new model will be slightly more expensive than the original model. In practice the polar residues (Thr, Ser, Asn, Gln) only constitute a very small fraction of a protein, which is itself usually only a small part of the simulation system. The additional costs will thus be negligible. However, the polarized particles require the use of the polarizable version of Martini water, which slows down the computation by up to a factor of 3 (for systems largely composed of water). Hence, in practice, the use of polarized particles and off-center charged particles should depend on the presumed importance of polar and charged residues in the system of interest. Whether or not the concept of polarized particles can be used to replace polar particles in general, i.e., also as part of other biomolecules, is currently under investigation. Preliminary endeavors aimed at reproducing membrane poration energies and transition states consistent with all-atom results, a known shortcoming of the Martini lipid model,[151] did not show much improvement yet.

3.4. Improving the Backbone of α-Helices and the Stability of poly-Ala and poly-Gly Sequences. In the Martini 2.1 protein force field,[14] the bonded interactions (bond lengths, bond angles, dihedral angles) were parametrized to match as closely as possible the corresponding distributions extracted from the protein data bank (PDB) for a large number of protein structures (ca. 2000). To obtain a good agreement of the relaxed CG structures with those from the PDB, the bonded parameters for the polypeptide backbone need to depend on the secondary structure. This dependency was implemented in the model through the equilibrium values and force constants of the angles and dihedrals between consecutive backbone beads, which differ for helical, extended, or coiled structures (Table 3 in Monticelli et al.[14]). For the bond between two neighboring backbone beads, the force constant was also made dependent on the secondary structure, whereas the equilibrium bond length was set to 0.35 nm in Martini 2.1, irrespective of the secondary structure. However, from the distance distribution extracted from the PDB (Figure 3a in Monticelli et al.[14]), it is clear that this approximation may hold quite well for extended and coiled structures, but the distribution between two backbone beads in helices peaks at a shorter distance of about 0.31 nm. In the new Martini 2.2 force field described in this work, the distance between two neighboring backbone beads in helical structures is set to 0.31 nm and treated by a constraint instead of a flexible harmonic bond. This setup more accurately describes the length of helical structures (see below) and is also more consistent with the secondary structure dependence of the other bonded parameters (angles, dihedrals).

Figure 4 shows the length distributions obtained from 100-ns MD simulations of a $(Leu)_{17}$ α-helix (T = 300 K, gas phase). This poly-Leu repeat was used as a representative example of a stable α-helix; however, the described effect is general and not restricted to certain amino acids. In the CG simulations, the helicity was imposed on the entire structure via the dihedral angles, which is the standard procedure used in the Martini force field. In the all-atom simulation, the CHARMM27 force field[152] with the CMAP[153] correction was used. The α-helical structure was stable throughout the 100 ns, with some transient fraying of the terminal 1−2 residues. Thus, to compare all-atom and CG simulations, we analyzed the distance between the backbone of residues 3 and 15. Prior to analysis, the all-atom trajectory was converted to the CG representation, although the difference between the backbone−backbone and Cα−Cα length distributions was negligible. Figure 4 shows that the

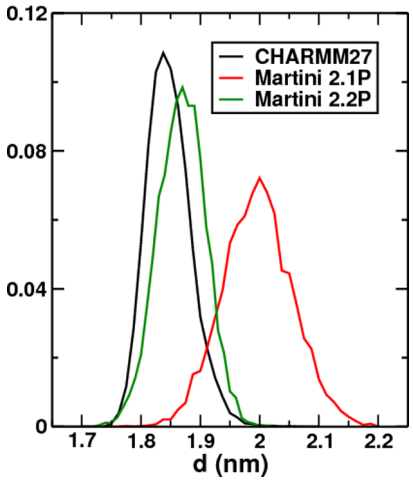

Figure 4. Probability distribution of the length of a $(Leu)_{17}$ α-helix obtained from all-atom simulation (CHARMM27, black curve) and from Martini 2.1/2.2 CG simulations (red/green curves). The length is estimated from the distance (d) between the backbone of Leu3 and Leu15.

Martini 2.1 force field yields too long α-helices (average distance 1.99 nm, red curve) as compared to the all-atom simulation (1.84 nm, black curve), due to the too large distance between neighboring backbone beads. In addition, the CG structure appears to be slightly too flexible, with a standard deviation of the distance distribution of 0.06 nm as compared to 0.04 nm in the all-atom simulation. Introducing a constraint bond length of 0.31 nm in Martini 2.2 (green curve) brings both the average (1.86 nm) as well as the width of the distribution (standard deviation 0.04 nm) into good agreement with the all-atom results.

Another issue pertains to the behavior of poly-Ala and Gly repeats. In the original parametrization of Martini 2.1, the value of the force constant (K_{BB}) used in the harmonic potential of the backbone−backbone bond is a function of the secondary structure of the residues. The relative flexibility of the loop regions (where coil, bend, and turn classification are often found) was modeled by a small K_{BB}. This increased flexibility of the bonded terms goes with the increased nonbonded interactions of the same secondary structure types. For instance, the coil and bend backbone particle type are P5 that has a very strong self-interaction. This combination of bonded and nonbonded parameters led in some specific cases to the local collapse of the protein backbone most often causing numerical instability. The collapse of the backbone results from the 1−3 nonbonded (LJ) interactions taking over the 1−2 and 2−3 (weakened) bonded terms. In most cases, the presence of a side chain bead prevents backbone beads from coming close. However, in cases in which two Gly and Ala residues are consecutive, the bond between them would collapse to a value of about 0.1 nm. The solution adopted in Martini 2.2 is the systematic increase of K_{BB} in the coil/turn/bend secondary structure type from 200/400/500 to 1250 kJ mol^{-1} nm^{-2}. This prevents the collapse of the bonds of consecutive Gly and Ala. To compensate for the associated decrease of flexibility, the bending angle applied to three consecutive backbone beads in coil/turn/bend is reduced from 25 to 20 kJ mol^{-1}. The new setup was tested on pentapeptides with sequences AlaAlaAlaAlaAla, AlaAlaValAlaAla, and AlaAlaAlaAlaVal and proved to be stable over microsecond time scales using

dx.doi.org/10.1021/ct300646g | J. Chem. Theory Comput. XXXX, XXX, XXX−XXX

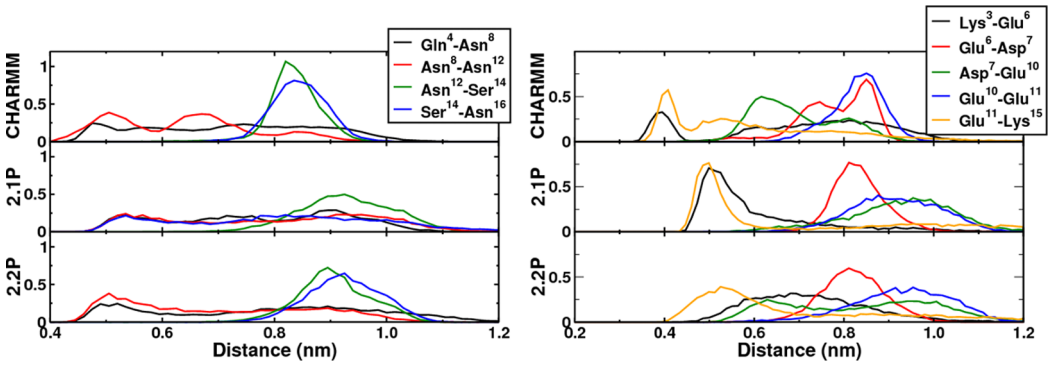

Figure 5. Distance distribution of the side chains of pairs of polar (left) and pairs of charged residues (right) that are part of the small helical GCN4 peptide. The distributions for the old Martini 2.1P, the new Martini 2.2P, and the all-atom CHARMM27 force field are compared.

conventional simulation setups. It is important to note that this parametrization of the flexible part of proteins applies to folded proteins and should not be taken as general parametrization for flexible protein regions such as large unfolded domains or intrinsically disordered proteins. In such cases, we expect that a more elaborated parametrization would be required.

3.5. Testing of New Parameters on a Soluble Peptide. To test the behavior of the new class of polarized and charged particles in a soluble peptide, we ran simulations of a small 16 residue helical peptide based on the N-terminal helix of the GCN4 leucine zipper (PDB entry code: 2ZTA). Residues 8 (Lys) and 12 (Leu) were mutated to polar Asn, bringing the total to five polar residues (Gln4, Asn8, Asn12, Ser14, Asn16) and six charged residues (Lys3, Glu6, Asp7, Glu9, Glu10 and Lys14), modeled as polarized and off-center charge particles, respectively. The helical conformation was restrained by using the standard Martini bonded potentials for α-helices with the changes proposed in the current work. Figure 5 shows the histograms of the COM distances between pairs of polar (left panel) and charged (right panel) side chains. The results are compared to a fully atomistic simulation using the CHARMM27 force field[152] with the CMAP corrections[153] and to Martini 2.1P. For the polar residues, there are two main differences between the Martini 2.1P and Martini 2.2P. First, the peaks observed at short distances (side chains pointing toward each other) and large distances (side chains pointing away from each other) shift to a smaller average distance in Martini 2.2P, thus better matching the position of the peaks obtained from the atomistic simulations. Second, the distributions of the pairs (Asn12−Ser14 and Ser14−Asn16) become narrower. However, the peak found at $d \approx 0.65$ nm (side chains pointing in the same direction) in the atomistic Asn8−Asn12 pair is still not observed in the CG simulations. In the case of the charged side chains, the situation is less clear. For the oppositely charged Lys3−Glu6 and Glu11−Lys15 pairs, the peak observed at a short distance becomes broader or completely disappears when using Martini 2.2P. For the oppositely (Glu6−Asp7) and equally charged (Glu10−Glu11) direct neighbors, the same orientations are sampled with the new parameters. For the oppositely charged Asp7−Glu10 pair, a new orientation at close distance is sampled, thus better reproducing the atomistic distribution.

Although the overall behavior of the side chains for this particular peptide appear to have improved with our new model, it is also clear that our CG model cannot capture some of the fine details of the distributions as seen when using an atomistic model. Additional testing is required to assess whether or not the Martini model can be further improved in this respect.

3.6. Implementation. To facilitate the use of the Martini force field, an auxiliary program was developed called *martinize.py*. This program offers a one-step solution for coarse-graining atomistic structures, yielding coarse-grained structures and corresponding topologies. The program contains easily editable tables for mapping atoms to CG beads and for assigning atom types and bonded parameters based on residue and secondary structure type. The secondary structure of a protein sequence can be specified explicitly or can be inferred from the structure by a call to the DSSP program.[154] Other features include the possibility of specifying disulfide bridges, adding arbitrary links between beads, and support for writing structures and topology files using the Elnedyn[155] approach. The *martinize.py* script can be downloaded from http://cgmartini.nl.

The user can also specify the version of the Martini force field that is used: Martini 2.1 or 2.2 with standard water or 2.1P and 2.2P in combination with polarizable water. The default of Martini 2.2P will be the use of polarized particles to model polar side chains and the charge off-center model for charged side chains. Both setups can be optionally reverted to regular particle types. A full list of parameters, indicating the changes between the previous and current versions of the protein force field, is provided as Supporting Information.

4. CONCLUSIONS

On the basis of recent data in which the Martini protein force field was compared to all-atom force fields and experimental data, we reparameterized a number of side chains. For Phe, we now use the SC5 particle type that makes this aromatic residue slightly more polar. Similarly, Trp behavior is improved with the new SC5-SC5-SC4-SNd assignment. For Pro, the side chain is made slightly more polar (C3), and at the same time the polarity of the backbone bead is increased (P4). Furthermore, we introduced a class of polarized particles to model the polar but neutral Asn, Gln, Ser, and Thr residues. This greatly improves their dimerization free energy in low dielectric solvents. We also presented a new model for charged residues with an off-center charge. This leads to an improvement of the potentials of mean force between two oppositely charged residues in an apolar medium. Both the polarized particle types and charge offset models should be used in combination with the polarizable Martini water model. Finally, we changed some of the bonded parameters to provide a better description of the length of an α-helix and to improve on numerical stability of

Gly and Ala repeats. All systems simulated in this study are stable with time steps up to at least 20 fs.

The changes described in the current paper, combined with the parameters from versions 2.1 and 2.1P that have not changed, define version 2.2 and 2.2P of the Martini protein force field. The new protein force field is still fully compatible with the Martini 2.0 lipid and carbohydrate force fields. A generic script has been developed in which these changes are implemented, allowing for a straightforward setup of CG simulations based on an atomistic input structure. Further testing is required to verify whether or not the changes proposed here are generic improvements. With the help of many Martini users around the globe, we are constantly trying to further optimize the model. Planned changes include a change in form of the nonbonded interaction potential to improve the surface tension of polar solvents and reduce the general over structuring seen with the current force field, as well as the introduction of polarized particles in the peptide backbone that will allow secondary structure transitions to occur.

■ ASSOCIATED CONTENT

Ⓢ Supporting Information

Mapping of the amino acids; backbone particle type in different kinds of secondary structures; backbone bonded parameters used in amino acid side chains; equilibrium bond length and force constant used in amino acid side chains; equilibrium angles, improper dihedral angles, and force constants used in amino acid side chains; and dummy bead bonded interactions for charged and polar side chains in the Martini 2.2P force field. This material is available free of charge via the Internet at http://pubs.acs.org.

■ AUTHOR INFORMATION

Corresponding Author

*E-mail: s.j.marrink@rug.nl.

Notes

The authors declare no competing financial interest.

■ ACKNOWLEDGMENTS

The authors would like to thank the many people that have directly and indirectly contributed to the development of the Martini force field. Funding from The Netherlands Organisation for Scientific Research (NWO) to S.J.M., L.V.S., and X.P. is greatly acknowledged. D.P.T. is an Alberta Innovates Health Solutions (AIHS) Scientist and Alberta Innovates Technology Futures Strategic Chair in (Bio)Molecular Simulation. W.F.D.B. is supported by an AIHS studentship. G.S. is an AIHS Postdoctoral Fellow. This work was supported by the Natural Sciences and Engineering Research Council of Canada (D.P.T.). Calculations were carried out in part on WestGrid/Compute Canada facilities.

■ REFERENCES

(1) Voth, G. A. *Coarse-Graining of Condensed Phase and Biomolecular Systems*; CRC Press: Boca-Raton, 2008.
(2) Padding, J. T.; Briels, W. J. *J. Phys. Cond. Matter* **2011**, *23*, 233101.
(3) Deserno, M. *Macr. Rap. Comm.* **2009**, *30*, 752−771.
(4) Clementi, C. *Curr. Op. Struct. Biol.* **2008**, *18*, 10−15.
(5) Klein, M. L.; Shinoda, W. *Science* **2008**, *321*, 798−800.
(6) Lyubartsev, A. P.; Laaksonen, A. *Phys. Rev. E.* **1995**, *52*, 3730.
(7) Reith, D.; Putz, M.; Muller-Plathe, F. *J. Comput. Chem.* **2003**, *24*, 1624.
(8) Izvekov, S.; Violi, A.; Voth, G. A. *J Phys Chem B* **2005**, *109*, 17019−17024.
(9) Noid, W. G.; Chu, J. W.; Ayton, G. S.; Krishna, V.; Izvekov, S.; Voth, G. A.; Das, A.; Andersen, H. C. *J. Chem. Phys.* **2008**, *128*, 244114.
(10) Brini., E.; van der Vegt, N. F. A. *J. Chem. Phys.* **2012**, *137*, 154113.
(11) Chaimovich, A.; Shell, M. S. *J. Chem. Phys.* **2011**, *134*, 094112.
(12) Marrink, S. J.; de Vries, A. H.; Mark, A. E. *J. Phys. Chem. B* **2004**, *108*, 750−760.
(13) Marrink, S. J.; Risselada, H. J.; Yefimov, S.; Tieleman, D. P.; de Vries, A. H. *J. Phys. Chem. B* **2007**, *111*, 7812−7824.
(14) Monticelli, L.; Kandasamy, S. K.; Periole, X.; Larson, R. G.; Tieleman, D. P.; Marrink, S. J. *J. Chem. Theory Comput.* **2008**, *4*, 819−834.
(15) Chu, J. W.; Ayton, G. S.; Izvekov, S.; Voth, G. A. *Mol. Phys.* **2007**, *105*, 167−175.
(16) Nielsen, S.; Bulo, R.; Moore, P.; Ensing, B. *Phys. Chem. Chem. Phys.* **2010**, *12*, 12401.
(17) Rzepiela, A. J.; Louhivuori, M.; Peter, C.; Marrink, S. J. *Phys. Chem. Chem. Phys.* **2011**, *13*, 10437−10448.
(18) Peter, C.; Kremer, K. *Soft Matter* **2009**, *5*, 4357−4366.
(19) Kamerlin, S. C. L.; Warshel, A. *Phys. Chem. Chem. Phys.* **2011**, *13*, 10401−10411.
(20) Yesylevskyy, S. O.; Schäfer, L. V.; Sengupta, D.; Marrink, S. J. *PLoS. Comput. Biol.* **2010**, *6*, e1000810.
(21) Wu, Z.; Cui, Q.; Yethiraj, A. J. *Phys. Chem. B* **2010**, *114*, 10524−10529.
(22) Dahlberg, M. *J. Phys. Chem. B* **2007**, *111*, 7194−7200.
(23) Perlmutter, J. D.; Sachs, J. N. *J. Am. Chem. Soc.* **2009**, *131*, 16362−16363.
(24) Lopez, C. A.; Rzepiela, A. J.; de Vries, A. H.; Dijkhuizen, L.; Hunenberger, P. H.; Marrink, S. J. *J. Chem. Theory Comput.* **2009**, *5*, 3195−3210.
(25) Wohlert, J.; Berglund, L. A. *J. Chem. Theory Comput.* **2011**, *7*, 753−760.
(26) Lee, H.; de Vries, A. H.; Marrink, S. J.; Pastor, R. W. *J. Phys. Chem. B* **2009**, *113*, 13186−13194.
(27) Rossi, G.; Monticelli, L.; Puisto, S. R.; Vattulainen, I.; Ala-Nissila, T. *Soft Matter* **2011**, *7*, 698−708.
(28) Hatakeyama, M.; Faller, R. *Phys. Chem. Chem. Phys.* **2007**, *9*, 4662−4672.
(29) Milani, A.; Casalegno, M.; Castiglioni, C.; Raos, G. *Macromol. Th. Sim.* **2011**, *20*, 305−319.
(30) Khalid, S.; Bond, P. J.; Holyoake, J.; Hawtin, R. W.; Sansom, M. S. P. *J. Roy. Soc Interface* **2008**, *5*, S241−S250.
(31) Wong-Ekkabut, J.; Baoukina, S.; Triampo, W.; Tang, I. M.; Tieleman, D. P.; Monticelli, L. *Nat. Nanotechnol.* **2008**, *3*, 363−368.
(32) Wallace, E. J.; Sansom, M. S. P. *Nanotechnology* **2009**, *20*, 045101.
(33) Monticelli, L. *J. Chem. Theory Comput.* **2012**, *8*, 1370−1378.
(34) Lee, H.; Larson, R. G. *J. Phys. Chem. B* **2008**, *112*, 7778−7784.
(35) Lee, H.; Choi, J. S.; Larson, R. G. *Macromolecules* **2011**, *44*, 8681−8686.
(36) Baoukina, S.; Tieleman, D. P. *Biophys. J.* **2010**, *99*, 2134−2142.
(37) Risselada, H. J.; Kutzner, C.; Grubmüller, H. *ChemBioChem* **2011**, *12*, 1049−1055.
(38) Risselada, H. J.; Marelli, G.; Fuhrmans, M.; Smirnova, Y. G.; Grubmüller, H.; Marrink, S. J.; Muller, M. *PLoS ONE* **2012**, *7*, e38302.
(39) Risselada, H. J.; Marrink, S. J. *Proc. Natl Acad. Sci. USA* **2008**, *105*, 17367−17372.
(40) Schäfer, L. V.; Marrink, S. J. *Biophys. J.* **2010**, *99*, L91−L93.
(41) Perlmutter, J. D.; Sachs, J. N. *J. Am. Chem. Soc.* **2011**, *133*, 6563−6577.
(42) Risselada, H. J.; Marrink, S. J.; Muller, M. *Phys. Rev. Lett.* **2011**, *106*, 148102.

(43) Muddana, H. S.; Chiang, H. H.; Butler, P. J. *Biophys. J.* **2012**, *102*, 489−497.
(44) Rosetti, C.; Pastorino, C. *J. Phys. Chem. B* **2012**, *116*, 3525−3537.
(45) Baoukina, S., Mendez-Villuendas, E., Bennett, W. F. D., Tieleman, D. P. *Faraday Disc.*, 2013, in press. DOI:10.1039/c2fd20117h
(46) Baoukina, S.; Mendez-Villuendas, E.; Tieleman, D. P. *J. Am. Chem. Soc.* **2012**, *134*, 17543−17553.
(47) Bennett, W. F. D.; MacCallum, J. L.; Hinner, M. J.; Marrink, S. J.; Tieleman, D. P. *J. Am. Chem. Soc.* **2009**, *131*, 12714−12720.
(48) Ogushi, F.; Ishitsuka, R.; Kobayashi, T.; Sugita, Y. *Chem. Phys. Lett.* **2012**, *522*, 96−102.
(49) Risselada, H. J.; Marrink, S. J. *Soft Matter* **2009**, *5*, 4531−4541.
(50) Sangwai, A. V.; Sureshkumar, R. *Langmuir* **2011**, *27*, 6628−6638.
(51) Velinova, M.; Sengupta, D.; Tadjer, A. V.; Marrink, S. J. *Langmuir* **2011**, *27*, 14071−14077.
(52) Rodgers, J. M.; Sørensen, J.; de Meyer, F. J. M.; Schiøtt, B.; Smit, B. *J. Phys. Chem. B* **2012**, *116*, 1551−1569.
(53) Kraft, J. F.; Vestergaard, M.; Schiøtt, B.; Thøgersen, L. *J. Chem. Theory Comput.* **2012**, *8*, 1556−1569.
(54) Tetsuro, N.; Ryuichi, U.; Yuko, O. *J. Phys. Soc. Jpn.* **2012**, *81*, 024002.
(55) Baoukina, S.; Monticelli, L.; Risselada, H. J.; Marrink, S. J.; Tieleman, D. P. *Proc. Natl. Acad. Sci. U.S.A.* **2008**, *105*, 10803−10808.
(56) Duncan, S. L.; Larson, R. G. *BBA-Biomembr.* **2010**, *1798*, 1632−1650.
(57) Kulovesi, P.; Telenius, J.; Koivuniemi, A.; Brezesinski, G.; Rantamaki, A.; Viitala, T.; Puukilainen, E.; Ritala, M.; Wiedmer, S. K.; Vattulainen, I.; Holopainen, J. M. *Biophys. J.* **2010**, *99*, 2559−2567.
(58) Baoukina, S.; Marrink, S. J.; Tieleman, D. P. *Biophys. J.* **2012**, *102*, 1866−1871.
(59) Fuhrmans, M.; Knecht, V.; Marrink, S. J. *J. Am. Chem. Soc.* **2009**, *131*, 9166−+.
(60) Rzepiela, A.; Sengupta, D.; Goga, N.; Marrink, S. J. *Farad. Discuss* **2010**, *144*, 431−443.
(61) Polyansky, A. A.; Ramaswarny, P. E.; Volynsky, P. E.; Sbalzarini, I. F.; Marrink, S. J.; Efremov, R. G. *J. Phys. Chem. Lett.* **2010**, *1*, 3108−3111.
(62) Khalfa, A.; Tarek, M. *J. Phys. Chem. B* **2010**, *114*, 2676−2684.
(63) Woo, H. J.; Wallqvist, A. *J. Phys. Chem. B* **2011**, *115*, 8122−8129.
(64) Thogersen, L.; Schiott, B.; Vosegaard, T.; Nielsen, N. C.; Tajkhorshid, E. *Biophys. J.* **2008**, *95*, 4337−4347.
(65) Arkhipov, A.; Yin, Y.; Schulten, K. *Biophys. J.* **2008**, *95*, 2806−2821.
(66) von Deuster, C. I. E.; Knecht, V. *BBA Biomembr.* **2011**, *1808*, 2867−2876.
(67) Fuhrmans, M.; Marrink, S. J. *J. Am. Chem. Soc.* **2012**, *134*, 1543−1552.
(68) Horn, J. N.; Sengillo, J. D.; Lin, D.; Romo, T. D.; Grossfield, A. *BBA Biomembr.* **2012**, *1818*, 212−218.
(69) Santo, K. P.; Berkowitz, M. L. *J. Phys. Chem. B* **2012**, *116*, 3021−3030.
(70) Davies, K. M.; Anselmi, C.; Wittig, I.; Faraldo-Gomez, J. D.; Kuhlbrandt, W. *Proc. Natl. Acad. Sci. U.S.A.* **2012**, *109*, 13602−13607.
(71) Khelashvili, G.; Albornoz, P. B. C.; Johner, N.; Mondal, S.; Caffrey, M.; Weinstein, H. *J. Am. Chem. Soc.* **2012**, *134*, 15858−15868.
(72) Periole, X.; Huber, T.; Marrink, S. J.; Sakmar, T. P. *J. Am. Chem. Soc.* **2007**, *129*, 10126−10132.
(73) Sengupta, D.; Marrink, S. J. *Phys. Chem. Chem. Phys.* **2010**, *12*, 12987−12996.
(74) Psachoulia, E.; Marshall, D. P.; Sansom, M. S. P. *Acc. Chem. Res.* **2010**, *43*, 388−396.
(75) Schäfer, L. V.; de Jong, D. H.; Holt, A.; Rzepiela, A. J.; de Vries, A. H.; Poolman, B.; Killian, J. A.; Marrink, S. J. *Proc. Natl. Acad. Sci. U.S.A.* **2011**, *108*, 1343−1348.
(76) Hung, A.; Yarovsky, I. *Biochem.* **2011**, *50*, 1492−1504.
(77) Stansfeld, P. J.; Hopkinson, R.; Ashcroft, F. M.; Sansom, M. S. P. *Biochem.* **2009**, *48*, 10926−10933.
(78) van den Bogaart, G.; Meyenberg, K.; Risselada, H. J.; Amin, H.; Willig, K. I.; Hubrich, B. E.; Dier, M.; Hell, S. W.; Grubmuller, H.; Diederichsen, U.; Jahn, R. *Nature* **2011**, *479*, 552−555.
(79) Domanski, J.; Marrink, S. J.; Schäfer, L. V. *BBA Biomembr.* **2012**, *1818*, 984−994.
(80) Koivuniemi, A.; Vuorela, T.; Kovanen, P. T.; Vattulainen, I.; Hyvönen, M. T. *PLoS Comput Biol* **2012**, *8*, e1002299.
(81) Janosi, L.; Li, Z.; Hancock, J. F.; Gorfe, A. A. *Proc. Natl. Acad. Sci. U.S.A.* **2012**, *109*, 8097−8102.
(82) Yin, F.; Kindt, J. T. *Biophys. J.* **2012**, *102*, 2279−2287.
(83) de Jong, D. H., Lopez, C. A., Marrink, S. J. *Farad. Discuss.* 2013, in press. DOI:10.1039/C2FD20086D
(84) Karo, J.; Peterson, P.; Vendelin, M. *J. Biol. Chem.* **2012**, *287*, 7467−7476.
(85) Periole, X.; Knepp, A. M.; Sakmar, T. P.; Marrink, S. J.; Huber, T. *J. Am. Chem. Soc.* **2012**, *134*, 10959−10965.
(86) Lumb, C. N.; Sansom, M. S. P. *PLoS Comput. Biol.* **2012**, *8*, e1002617.
(87) Hall, B. A.; Armitage, J. P.; Sansom, M. S. P. *PLoS Comput. Biol.* **2012**, *8*, e1002685.
(88) Johnston, J. M.; Wang, H.; Provasi, D.; Filizola, M. *PLoS Comput. Biol.* **2012**, *8*, e1002649.
(89) Sengupta, D.; Chattopadhyay, A. J. *Phys. Chem. B* **2012**, *116*, 12991−12996.
(90) Louhivuori, M.; Risselada, H. J.; van der Giessen, E.; Marrink, S. J. *Proc. Natl. Acad. Sci. U.S.A.* **2010**, *107*, 19856−19860.
(91) Lycklama, J. A.; Bulacu, M.; Marrink, S. J.; Driessen, A. J. M. *J. Biol. Chem.* **2010**, *285*, 23747−23754.
(92) Anselmi, C.; Grininger, M.; Gipson, P.; Faraldo-Gomez, J. D. *J. Am. Chem. Soc.* **2010**, *132*, 12357−12364.
(93) Cojocaru, V.; Balali-Mood, K.; Sansom, M. S. P.; Wade, R. C. *PLoS Comput. Biol.* **2011**, *7*, e1002152.
(94) Hall, B. A.; Armitage, J. P.; Sansom, M. S. P. *PLoS Comp. Biol.* **2011**, *7*, e1002204.
(95) Nagarajan, A.; Andersen, J. P.; Woolf, T. B. *Proteins* **2012**, *80*, 1929−1947.
(96) Deplazes, E.; Louhivuori, M.; Jayatilaka, D.; Marrink, S. J.; Corry, B. *PLoS Comp. Biol.* **2012**, *8*, e1002683.
(97) Zhang, L.; Bai, S.; Sun, Y. *J. Mol. Graph. Modell.* **2011**, *29*, 906−914.
(98) Hung, A.; Mwenifumbo, S.; Mager, M.; Kuna, J. J.; Stellacci, F.; Yarovsky, I.; Stevens, M. M. *J. Am. Chem. Soc.* **2011**, *133*, 1438−1450.
(99) Gautieri, A.; Russo, A.; Vesentini, S.; Redaelli, A.; Buehler, M. J. *J. Chem. Theory Comput.* **2010**, *6*, 1210−1218.
(100) Li, T., Gu, Y. T., Oloyede, A., Yarlagadda, P. K. D. V. *Comput. Meth. Biomech. Biomed. Eng.* 2012, in press. DOI:10.1080/10255842.2012.706279
(101) Frederix, P. W. J. M.; Ulijn, R. V.; Hunt, N. T.; Tuttle, T. *J. Phys. Chem. Lett.* **2011**, *2*, 2380−2384.
(102) Guo, C.; Luo, Y.; Zhou, R.; Wei, G. *ACS Nano* **2012**, *6*, 3907−3918.
(103) Gudlur, S.; Sukthankar, P.; Gao, J.; Avila, L. A.; Hiromasa, Y.; Chen, J.; Iwamoto, T.; Tomich, J. M. *PLoS ONE* **2012**, *7*, e45374.
(104) Lee, O. S.; Cho, V.; Schatz, G. C. *Nano Lett.* **2012**, *12*, 4907−4913.
(105) Sorensen, J.; Periole, X.; Skeby, K. K.; Marrink, S. J.; Schiott, B. *J. Phys. Chem. Lett.* **2011**, *2*, 2385−2390.
(106) Seo, M.; Rauscher, S.; Pomès, R.; Tieleman, D. P. *J. Chem. Theory Comput.* **2012**, *8*, 1774−1785.
(107) Stukan, M. R.; Ligneul, P.; Crawshaw, J. P.; Boek, E. S. *Langmuir* **2010**, *26*, 13342−13352.
(108) Sergi, D.; Scocchi, G.; Ortona, A. *J. Chem. Phys.* **2012**, *137*, 094904.
(109) Titov, A. V.; Kral, P.; Pearson, R. *ACS Nano* **2010**, *4*, 229−234.
(110) Ramalho, J. P. P.; Gkeka, P.; Sarkisov, L. *Langmuir* **2011**, *27*, 3723−3730.
(111) Patra, N.; Kral, P. *J. Am. Chem. Soc.* **2011**, *133*, 6146−6149.

(112) Song, B.; Yuan, H. J.; Jameson, C. J.; Murad, S. *Mol. Phys.* **2011**, *109*, 1511−1526.
(113) Kyrychenko, A.; Karpushina, G. V.; Bogatyrenko, S. I.; Kryshtal, A. P.; Doroshenko, A. O. *Comput. Theor. Chem.* **2011**, *977*, 34−39.
(114) Lin, L. Q.; Zheng, Y. G.; Zhang, H. W.; Chen., Z. *Langmuir* **2011**, *27*, 8323−8332.
(115) Lee, H.; Kim, H. *J. Phys. Chem. C* **2012**, *116*, 9327−9333.
(116) Bulacu, M.; Periole, X.; Marrink, S. J. *Biomacromolecules* **2012**, *13*, 196−205.
(117) Raudino, A.; Pannuzzo, M.; Karttunen, M. *J. Chem. Phys.* **2012**, *136*, 055101.
(118) Wang, S., Larson, R. G. *Soft Matter*, 2013, in press.. DOI: 10.1039/C2SM26850G
(119) Liu, C., Faller, R. *Langmuir*, 2012, in press. DOI:10.1021/la303511p
(120) Uttarwar, R. G., Potoff, J., Huang, Y. *Ind. Eng. Chem. Res.*, 2012, in press. DOI: 10.1021/ie301228f
(121) Berntsson, R. P. A.; Doeven, M. K.; Fusetti, F.; Duurkens, R. H.; Sengupta, D.; Marrink, S. J.; Thunnissen, A. M. W. H.; Poolman, B.; Slotboom, D. J. *EMBO J.* **2009**, *28*, 1332−1340.
(122) Shih, A. Y.; Freddolino, P. L.; Arkhipov, A.; Schulten, K. *J. Struct. Biol.* **2007**, *157*, 579−592.
(123) Vuorela, T. A.; Catte, A.; Niemela, P. S.; Hall, A.; Hyvonen, M. T.; Marrink, S. J.; Karttunen, M.; Vattulainen, I. *PLoS Comp. Biol.* **2010**, *6*, e1000964.
(124) Murtola, T.; Vuorela, T. A.; Hyvonen, M. T.; Marrink, S. J.; Karttunen, M.; Vattulainen, I. *Soft Matter* **2011**, *7*, 8135−8141.
(125) Perlmutter, J. D.; Drasler, W. J.; Xie, W.; Gao, J. L.; Popot, J. L.; Sachs, J. N. *Langmuir* **2011**, *27*, 10523−10537.
(126) Popovic, K.; Holyoake, J.; Pomès, R.; Privé, G. G. *Proc. Natl. Acad. Sci. U.S.A.* **2012**, *109*, 2908−2912.
(127) Ollila, O. H. S.; Lamberg, A.; Lehtivaara, M.; Koivuniemi, A.; Vattulainen, I. *Biophys. J.* **2012**, *103*, 1236−1244.
(128) Corsi, J.; Hawtin, R. W.; Ces, O.; Attard, G. S.; Khalid, S. *Langmuir* **2010**, *26*, 12119−12125.
(129) Ahmad, S.; Johnston, B. F.; Mackay, S. P.; Schatzlein, A. G.; Gellert, P.; Sengupta, D.; Uchegbu, I. F. *J. Royal Soc. Int.* **2010**, *7*, S423−S433.
(130) Winter, N. D.; Murphy, R. K. J.; O'Halloran, T. V.; Schatz, G. C. *J. Lipos. Res.* **2011**, *21*, 106−115.
(131) Peng, L. L. X.; Ivetac, A.; Chaudhari, A. S.; Van, S.; Zhao, G.; Yu, L.; Howell, S. B.; McCammon, J. A.; Gough, D. A. *Biopolymers* **2010**, *93*, 936−951.
(132) Peng, L. X.; Yu, L.; Howell, S. B.; Gough, D. A. *J. Chem. Inf. Model.* **2011**, *51*, 3030−3035.
(133) Lee, S. J.; Schlesinger, P. H.; Wickline, S. A.; Lanza, G. M.; Baker, N. A. *Soft Matter* **2012**, *8*, 3024−3035.
(134) Leung, A. K. K.; Hafez, I. M.; Baoukina, S.; Bellinveau, N. M.; Zhigaltsev, I.; Afshinmanesh, E.; Tieleman, D. P.; Hansen, C. L.; Hope, M. J.; Cullis, P. R. *J. Phys. Chem. C* **2012**, *116*, 18440−18450.
(135) Bond, P. J.; Holyoake, J.; Ivetac, A.; Khalid, S.; Sansom, M. S. P. *J. Struct. Biol.* **2007**, *157*, 593−605.
(136) Shih, A. Y.; Arkhipov, A.; Freddolino, P. L.; Schulten, K. *J. Phys. Chem. B* **2006**, *110*, 3674−3684.
(137) Singh, G.; Tieleman, D. P. *J. Chem. Theory Comput.* **2011**, *7*, 2316−2324.
(138) Wimley, W. C.; White, S. H. *Nat. Struct. Biol.* **1996**, *3*, 842−848.
(139) de Jong, D. H.; Periole, X.; Marrink, S. J. *J. Chem. Theory Comput.* **2012**, *8*, 1003−1014.
(140) MacCallum, J. L.; Bennett, W. F. D.; Tieleman, D. P. *Biophys. J.* **2008**, *94*, 3393−3404.
(141) Hess, B.; Kutzner, C.; van der Spoel, D.; Lindahl, E. *J. Chem. Theory Comput.* **2008**, *4*, 435−447.
(142) Marrink, S. J.; Periole, X.; Tieleman, D. P.; de Vries, A. H. *Phys. Chem. Chem. Phys.* **2010**, *12*, 2254−2256.
(143) Berendsen, H. J. C.; Postma, J. P. M.; van Gunsteren, W. F.; Dinola, A.; Haak, J. R. *J. Chem. Phys.* **1984**, *81*, 3684−3690.
(144) Kumar, S.; Bouzida, D.; Swendsen, R. H.; Kollman, P. A.; Rosenberg, J. M. *J. Comput. Chem.* **1992**, *13*, 1011−1021.
(145) Hess, B.; Holm, C.; van der Vegt, N. *J. Chem. Phys.* **2006**, *124*, 164509.
(146) de Jong, D. H.; Schäfer, L. V.; de Vries, A. H.; Marrink, S. J.; Berendsen, H. J. C.; Grubmüller, H. *J. Comput. Chem.* **2011**, *32*, 1919−1928.
(147) Hub, J. S.; de Groot, B. L.; van der Spoel, D. *J. Chem. Theory Comput.* **2010**, *6*, 3713−3720.
(148) Schwarzenbach, R. P., Gschwend, P. M., Imboden, D. M. *Envir. Org. Chem.*, John Wiley & Sons Inc.: New York, 2003.
(149) Radzicka, A.; Wolfenden, R. *Biochem.* **1988**, *27*, 1664−1670.
(150) Wolfenden, R.; Andersson, L.; Cullis, P. M.; Southgate, C. C. B. *Biochem.* **1981**, *20*, 849−855.
(151) Bennett, W. F. D.; Tieleman, D. P. *J. Chem. Theo. Comp.* **2011**, *7*, 2981−2988.
(152) MacKerell, A. D., Jr.; Banavali, N.; Foloppe, N. *Biopolymers* **2001**, *56*, 257−265.
(153) MacKerell, A. D., Jr.; Feig, M.; Brooks, C. L., III *J. Comput. Chem.* **2004**, *25*, 1400−1415.
(154) Kabsch, W.; Sander, C. *Biopolymers* **1983**, *22*, 2577−2637.
(155) Periole, X.; Cavalli, M.; Marrink, S. J.; Ceruso, M. A. *J. Chem. Th. Comp.* **2009**, *5*, 2531−2543.